Mesenchymal Stem Cells (MSC) Derived from Induced Pluripotent Stem Cells (iPSC) Equivalent to Adipose-Derived MSC in Promoting Intestinal Healing and Microbiome Normalization in Mouse Inflammatory Bowel Disease Model

SIRIKUL SOONTARARAK (ID), LYNDAH CHOW (ID), VALERIE JOHNSON, JONATHAN COY, WILLIAM WHEAT, DANIEL REGAN, STEVEN DOW

Center for Immune and Regenerative Medicine, Department of Clinical Sciences, College of Veterinary Medicine and Biomedical Sciences, Colorado State University, Fort Collins, Colorado, USA

Correspondence: Steven Dow, D.V.M., Ph.D., Department of Clinical Sciences, Colorado State University, Campus Delivery 1678, Fort Collins, Colorado 80523, USA. Tel: (970) 297-4014; e-mail: sdow@colostate.edu

ABSTRACT

Cellular therapy with allogeneic or autologous mesenchymal stem cells (MSC) has emerged as a promising new therapeutic strategy for managing inflammatory bowel disease (IBD). However, MSC therapy ideally requires a convenient and relatively homogenous cell source (typically bone marrow or adipose tissues) and the ability to generate cells with stable phenotype and function. An alternative means of generating allogeneic MSC is to derive them from induced pluripotent stem cells (iPSC), which could in theory provide an indefinite supply of MSC with well-defined phenotype and function. Therefore, we compared the effectiveness of iPSC-derived MSC (iMSC) and adipose-derived MSC (adMSC) in a mouse model of IBD (dextran sodium sulfate-induced colitis), and investigated mechanisms of intestinal protection. We found that iMSC were equivalent to adMSC in terms of significantly improving clinical abnormalities in treated mice and reducing lesion scores and inflammation in the gut. Administration of iMSC also stimulated significant intestinal epithelial cell proliferation, increased in the numbers of Lgr5+ intestinal stem cells, and increased intestinal angiogenesis. In addition, the microbiome alterations present in mice with colitis were partially restored to resemble those of healthy mice following treatment with iMSC or adMSC. Thus, iMSC administration improved overall intestinal health and healing with equivalent potency to treatment with adMSC. This therefore is the first report of the effectiveness of iMSC in the treatment of IBD, along with a description of unique mechanisms of action with respect to intestinal healing and microbiome restoration. STEM CELLS TRANSLATIONAL MEDICINE *2018;7:456–467*

SIGNIFICANCE STATEMENT

Current studies revealed the promising therapeutic mechanisms in Inflammatory Bowel Disease by which Mesenchymal Stem Cells (MSC) modulate not only an immunological action but also a regenerative effect on the intestinal epithelium normalization. The routine use of MSC cellular therapy with would benefit from a uniform cell source, with stable phenotype and function as well as providing a solution to potential safety issues. Therefore, this work provides strong support for the use of iPSC-derived MSC as a more uniform with well-defined phenotype and function as a sustainable source of cells which paves the way for a clinical application for IBD cellular therapy.

INTRODUCTION

Inflammatory bowel disease (IBD), including Crohn's disease and ulcerative colitis, results in intestinal inflammation due to immune dysregulation in the gut [1–4]. These diseases are characterized by infiltration of inflammatory cells and variable degrees of intestinal injury [5]. While substantial progress has been made in treating IBD with new immune modulatory drugs, there still remains a need for new approaches to treatment and management of the disease, especially treatments with few side effects and long duration of action.

Cellular therapy with immune-modulatory mesenchymal stem cells (MSC) has emerged as a promising new therapeutic strategy for managing IBD. For one, MSC are strongly immune modulatory, and suppress a number of different inflammatory processes [6–10]. Importantly, it has now been demonstrated in several studies in rodent models of IBD that systemic administration of MSC by the i.v. or i.p. routes can significantly

ameliorate intestinal inflammation [11–14]. Moreover, these same positive effects have also been observed in humans with Crohn's disease and ulcerative colitis treated with cellular therapy, and in a canine spontaneous animal model of IBD [15–21]. Thus, there is strong evidence that cellular therapy with MSC may be an effective management option for IBD, even in individuals with drug-refractory disease.

Despite the compelling evidence of the efficacy of cellular therapy for management of IBD, our understanding of the mechanisms by which MSC improve clinical and immunological abnormalities in the disease remains incomplete. For example, animal models of IBD (principally the dextran sodium sulfate (DSS)-induced colitis model) have demonstrated that MSC administration can reduce inflammatory cell infiltrates in the gut [13, 22–24]. There are conflicting data on the degree to which MSC actually localize to the gut following i.v. delivery, although the consensus seems to be that overall recruitment to the gut is relatively inefficient [13, 25, 26]. To date, most studies of MSC cellular therapy for IBD have focused on immune modulation by MSC. However, MSC are also suggested to have a stimulatory effect on the gut epithelium itself, including stimulation of intestinal stem cell proliferation in radiation-induced GI injury models [27–29].

However, despite the promise of cellular therapies, challenges remain in the application of cellular therapy as a viable option for management of IBD. For example, the source of MSC (whether autologous or allogeneic) is a major variable impacting the efficacy of therapy [30–32] as well as donor age [32–34] and donor-to-donor intrinsic MSC variability [35, 36]. Thus, the routine use of MSC cellular therapy with consistent benefit would benefit from a uniform cell source, with stable phenotype and function.

One solution to this problem of uniform cell sourcing is the use of MSC derived from induced pluripotent stem cells (iPSC). A number of studies have determined that iPSC-derived MSC (iMSC) closely resemble conventional bone marrow or adipose-tissue derived MSC in terms of both phenotype and function [37–40]. The ability of iMSC to suppress inflammation in vivo has also been demonstrated in mouse models, including allergic airway disease [38, 40, 41].

Therefore, in the present study, we investigated the effectiveness of iMSC for treatment of IBD, using a mouse model of DSS-induced colitis. Studies were done to investigate in greater detail the mechanisms by which MSC may ameliorate the intestinal abnormalities in IBD, including effects on intestinal healing and fecal microbiome populations, as well as inflammation. These studies revealed that iMSC were as effective as conventional, adipose-derived MSC (adMSC) for treatment of established and ongoing colitis in mice. In addition, these investigations also revealed important indirect stimulatory effects of MSC on intestinal healing and angiogenesis, as well as normalization of the intestinal microbiome. Taken together, these studies provide strong support for the use of iMSC as a more uniform and sustainable source of cells for IBD cellular therapy.

MATERIALS AND METHODS

The animal experiments described here were conducted under protocols reviewed and approved Institutional Animal Care and Use Committee at Colorado State University (IACUC; protocol number 15-6194A).

Animals

Female CD-1 mice (age 8 weeks, weighing 25–30 g) were purchased from Charles River Laboratories (Wilmington, MA).

Mice were housed under a 12 hours-light/12 hours-dark cycle and a constant temperature at 25°C and were provided the standard diet and water ad libitum until starting the experiment.

MSCs Isolation, Culture, and Tri-Lineage Differentiation

The MSCs used for this experiment were isolated from abdominal and inguinal adipose tissues of 10 weeks old female CD-1 mice under sterile conditions. Approximately 0.5 g of isolated fat was washed with sterile Dulbecco's phosphate-buffered saline (Sigma Aldrich, St. Louis, MO), then mechanically minced by scalpel blade and digested using collagenase (Sigma Aldrich; 1 mg/ml) for 30 minutes at 37°C. The stromal vascular fraction (SVF) was isolated by centrifugation at 380g for 5 minutes. After two washes with complete culture medium, the SVF was transferred into 75 cm^2 tissue culture flasks (Falcon, Thermo Fisher, Waltham, MA) and incubated at 37°C, 5% CO$_2$. After 72 hours, the flasks were washed to discard nonadherent cells, and refed with fresh complete medium. Proliferating colonies of adherent cells were allowed to reach 70% confluency, with medium changes every 48 hours. Thereafter, the cells were removed from flasks for passage by treating with trypsin (0.25% trypsin; EDTA, Gibco, Carlsbad, CA) and placed in 225 cm^2 flasks for further expansion. For studies reported here, adMSC were used at passage 3–4, and collected when approximately 80% confluent.

The iMSC line used in these studies was derived from a CD-1 mouse by the University of Colorado Denver Charles C. Gates Center for Regenerative Medicine and Stem Cell Biology iPSC Core. Transgene integration-free iPS cells were generated from mouse skin fibroblasts using a CytoTune iPS Reprograming kit (Life Technologies Corp. Grand Island, NY) according to manufacture instructions. The ability of adMSC and iMSC to undergo tri-lineage differentiation was assessed using a StemPro differentiation kit (Gibco). The phenotype of the differentiated cells was assessed by specific cytostaining (adipogenesis; Oil Red O, chondrogenesis; Alcian Blue, and osteogenesis; Alizarin Red).

Flow Cytometry

The surface phenotype of the adMSC and iMSC was determined as described previously [6]. Briefly, single cell suspensions were prepared at a concentration of 1×10^6 cells per ml in FACS buffer, and 1×10^5 cells were immunostained in single wells of round bottom 96-well plates (Corning Inc. Corning, NY). The primary antibodies were used as following; Sca-1-APC (clone eBR2a), CD11b-FITC (clone M1/70), CD29-biotin (clone HMb1-1), CD31-FITC (clone 390), CD44-FITC (clone IM7), CD45-PE (clone 30-F11), CD73-PE (clone eBioTY/11.8), CD90.2-eFlour 450 (clone 53-2.1), CD106-biotin (clone 429). All antibodies were obtained from eBioscience (San Diego, CA). For evaluation of leukocyte populations, the following primary antibodies were used: CD4-FITC (clone GK1.5), CD8-APC-e780 (clone 53-6.7), CD11c-FITC (clone N418), CD45-eFlour450 (clone 30-F11), FOXP3-PE (clone JFK-16s), B220-APC (RA3-682), Ly6G-APC-e780 (clone RB6-8C5), Ly6C-PE (clone HK1.4), F4/80-APC (clone BM8). In addition, intracellular staining was done using fixation permeabilization buffer for anti-FOXP3 staining (Thermo Fisher), after cell surface staining was done. Cells were evaluated using a Beckman Coulter Gallios flow cytometer (Brea, CA) and data were analyzed using FlowJo Software (Ashland, OR). An example of gating scheme is shown in Supporting Information Fig. S1.

DSS-Induced Colitis Model and Clinical Scoring of Disease Severity

Colitis was induced in mice using DSS administered at a concentration of 2.5% wt/vol in drinking water, as described previously [42]. Briefly, (DSS; Mr ∼40,000, Sigma-Aldrich, St. Louis, MO) by administered in drinking water daily throughout the study period. For each study, mice ($n = 5$ per group) were randomly assigned to the following groups: (a) untreated control group; (b) DSS treatment only; (c) DSS + adMSC administration; and (d) DSS + iMSC administration. Mice were monitored daily for body weight, clinical signs, stool consistency and color daily. On days 10, 13, and 16 of the study (with DSS administration initiated on day 0), MSC were administered by tail vein injection at a dose of 1×10^6 cells per mouse in 200 µl phosphate-buffered saline (PBS). The control and DSS only groups of mice were administered 200 µl of PBS by tail vein injection.

Clinical scoring was done using a modified scoring matrix, as described previously [13, 43]. Briefly, the mice were weighed, and fresh stool collected daily, and monitored for clinical signs every day. The percent weight loss was calculated daily and scored as 0 (no loss), −1 (1%–5%), −2 (5%–10%), −3 (10%–20%) and −4 for above 20%. Fecal occult blood was measured using a test kit (Fisher Healthcare, Houston, TX). The color reference guide was modified to quantitate the level of positive occult blood in a range of 0 (no blood), −1, −2, −3, and −4 with the darkest blue indicating the strongest positive reference color of the test kit. The fecal consistency scoring was 0 (normal), −1 (moist), −2 (loose stool), −3 (watery). The final clinical score was the sum of the scoring from weight, fecal color, and fecal consistency, and the possible maximum score was −12.

Sample Collection for Histology and Immunofluorescent Staining

Mice were euthanized on day 19 of the study (3 days after the last MSC injection) and the colon was removed and weighed and the length determined. A 1 cm section of colon was cut and frozen at −80°C. Half of the remaining colonic tissue was fixed in 10% neutral buffered formalin for standard histological processing, while the other half was proceeded for immunofluorescent staining by fixation in a 1% paraformaldehyde-lysine-periodate (PLP) solution (1% paraformaldehyde in 0.2M lysine-HCl, 0.1M anhydrous dibasic sodium phosphate, with 0.21% sodium periodate) (Fisher Scientific, Hampton, NH) for 24 hours at 4°C. Following PLP fixation, colonic tissues were placed in a 30% wt/vol sucrose solution for 24 hours at 4°C, prior to embedding and freezing in O.C.T. compound (Tissue Tek, Tokyo).

Histopathology

Formalin-fixed paraffin-embedded colon tissues were processed for histological evaluation by routine H&E staining. Histopathological scoring of colonic tissues was completed in a blinded fashion by a board-certified veterinary pathologist (DR). A previously published scoring system for colonic inflammation (score 1–6; two categories) [44] was modified to include a category for mucosal inflammation and damage as follows (score 1–3); 1 (leukocyte infiltration), 2 (mucosal erosion/ulceration +/− colonic gland ecatasia and necrosis), 3 (collapse of mucosal architecture +/− replacement granulation tissue). The final score was the summation of all parts of the scoring index, with a maximum possible score of 9.

Immunofluorescence Staining

PLP-fixed, OCT-embedded frozen tissues were cryosectioned at 5 µm thickness and mounted on Superfrost slides Fisher Scientific for immunofluorescent staining. The following primary antibodies were used for immunolabeling: CD11b (clone M1/70), F4/80 (clone BM8), CD3 (clone 145-2C11), CD4 (clone 4SM95), CD103 (clone 2E7; all from eBiocience), cytokeratin-20 (Abcam, Cambridge, MA), CD31 (clone MEC 13.3; BD Pharmingen); FOXP3 (clone JFK-16s), Ki-67 (clone SolA15; all from eBioscience), Lgr5 (Abcam); using 0.1% Triton X and 0.25% saponin (Sigma-Aldrich) as permeabilizing agent, with overnight incubation. Secondary antibodies were conjugated with Cy3 or Alexa Flour488 (1:200 in PBST, Jackson ImmunoResearch Laboratories). The tissue sections were washed and counter stained with DAPI (Molecular Probe, Eugene, OR). The slices were subsequently mounted with Prolong Diamond Antifade medium (Thermo Fisher, Waltham, MA) and placed under a coverslip. Appropriate isotype control mAbs were used for all studies. The tissues were visualized using an Olympus IX83 confocal microscope and Hamamatsu digital camera.

For quantitation of images by confocal microscopy, 10 fields (×20 objective magnification) of colonic mucosa were randomly sampled using the DAPI channel, and images were acquired. The positive fluorescent cells expressing FOXP3, CD11b, F4/80, CD3, CD4+ T cell (CD3+, CD4+), CD103, Ki-67, Lgr5, or CD31 were quantified per mm^2 of tissue. For calculation of microvessel density, the percentage of CD31 fluorescence area was divided by the total pixels of mucosal area of each image tile, using ImageJ software [45] (Supporting Information Fig. S2).

For MSC tracking studies, MSC were labeled with fluorescent DiR or with DiD dye (Invitrogen, Eugene, OR) and mice were imaged using an IVIS instrument (PerkinElmer, Waltham, MA).

Microbiome 16S rRNA Sequencing

Fecal pellet DNA extraction was performed using a Mobio Power-Soil DNA Isolation kit (Qiagen, Valencia, CA) according to manufactures instructions. Extracted DNA was submitted to Novogene Corporation (Chula Vista, CA) for 16S rRNA sequencing. According the company report of analysis, DNA concentration and purity was monitored on 1% agarose gels. 16S rRNA genes of V4 region were amplified using V4: 515F-806R. All PCR reactions were carried out with Phusion High-Fidelity PCR Master Mix (New England Biolabs, MA). PCR products were purified with Qiagen Gel Extraction Kit. Sequencing libraries were generated using TruSeq DNA PCR-Free Sample Preparation Kit (Illumina, San Diego, CA) following manufacturer's recommendations and index codes were added. The library quality was assessed on the Qubit@ 2.0 Fluorometer and Agilent Bioanalyzer 2100 system. The library was sequenced on an Illumina HiSeq 2500 platform and 250 bp paired-end reads were generated. Paired-end reads were assigned to samples based on their unique barcode and truncated by cutting off the barcode and primer sequence. Then quality filtering on the raw tags were performed according to the QIIME version 1.7.0. Chimeric sequences were removed using UCHIME Algorithm. Operational Taxonomic Units (OTUs) were conducted at 97% sequence similarity using QIIME for taxonomically classified. For genus level, naive Bayesian classifier retrained on the Green-Genes 16S rRNA gene database was used at 0.8 confidence threshold for taxonomic assignment. OTUs abundance information was normalized using a standard of sequence number corresponding to the sample with the least sequences. Alpha diversity
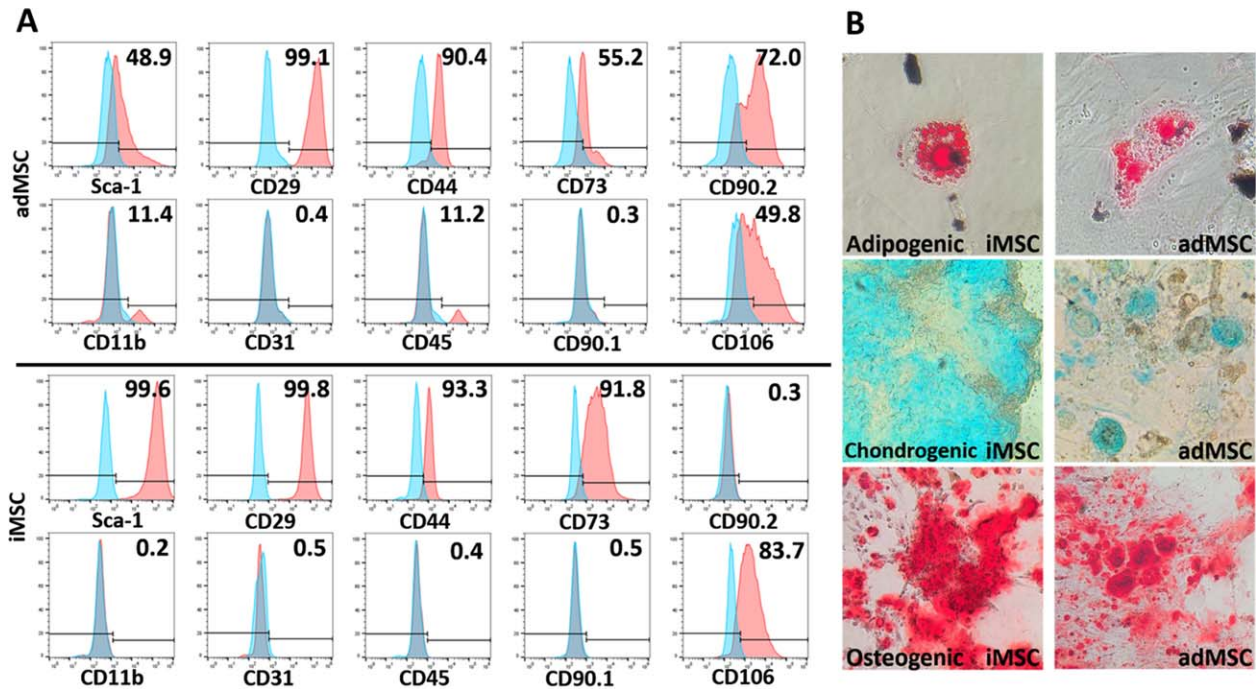
Figure 1. Phenotypic characterization of iMSC and adMSC. **(A):** Expression of cell surface determinants using flow cytometry. Specific antibody staining depicted in red, whereas isotype control staining for each displayed in blue. The percentage of the positive staining for each marker was indicated. **(B):** Tri-lineage differentiation of passage 3 MSC, as described in "Materials and Methods" section. Adipocytes detected using Oil Red O ($\times$200); chondrogenesis by Alcian Blue, and osteogenesis by Alizarin Red staining at day 12 after differentiation. Abbreviations: adMSC, adipose-derived mesenchymal stem cell; iMSC, iPSC-derived mesenchymal stem cells.

was calculated using Shannon diversity index. Beta diversity on both weighted and unweighted unifrac were calculated by QIIME software (Version 1.7.0).

Statistical Analysis

Data were analyzed using Prism 7 software (GraphPad, San Diego, CA) and results were shown as mean $\pm$ SD (unless otherwise stated) and statistical significant was set at $p < .05$. The normality of data was analyzed using Shapiro-Wilk normality test. The clinical score and histopathological inflammatory score data were transformed to normal distribution. Statistical differences between groups were evaluated using one-way ANOVA with multiple means comparisons using Tukey's adjustment or otherwise stated.

RESULTS

Phenotypic Characterization of iMSC and adMSC

Both iMSC and adMSC were assessed for MSC characteristics and identification criteria, as established by the International Society for Cellular Therapy [46]. Flow cytometric analysis revealed high expression of MSC markers, including Sca-1, CD29, CD44, CD73, and CD106. In contrast, there was no expression of leukocyte markers, including CD45, CD11b, and CD31 (Fig. 1A). We found that whereas adMSC highly expressed CD90, the iMSC were negative for CD90 expression. Both cell types were positive for expression of CD106, which was expressed exclusively on MSC and not on skin fibroblasts (not shown). Tri-lineage differentiation studies also revealed that both adMSC and iMSC could be differentiated into adipocytes, osteoblasts, and chondrocytes (Fig. 1B).

Effects of MSC Administration on Clinical Signs and Colonic Lesions in Mice with DSS-Induced Colitis

Mice treated with DSS in their drinking water exhibited clinical signs consistent with colitis, including sustained weight loss, bloody diarrhea and abnormal fecal consistency resulting in decreased clinical scores over time (Fig. 2). Following the onset of signs of colitis, mice ($n = 5$ per treatment group) were treated with MSC (1×10^6 MSC per mouse per injection, i.v.) on days 10, 13, and 16. In mice treated with either iMSC or adMSC; the clinical illness scores were significantly reduced compared to mice treated with DSS only (for iMSC-treated mice, $p = .003$ and for adMSC treated mice, $p = .001$ respectively) (Fig. 2A). The improvement in clinical scores became apparent within 1 day of the first MSC injection and was maintained during the period of MSC injections, whereas clinical scores continued to worsen in DSS-only treated animals.

Gross lesion scores and histopathology were evaluated in distal colon tissues collected in mice euthanized at 72 hours after the third MSC injection (day 19 of DSS treatment). In mice treated with DSS only (compared to untreated control animals), the colon appeared shortened and hyperemic (data not shown). Histologically, colonic tissues from DSS-treated mice exhibited severe infiltration of inflammatory cells, variable degrees of colonic gland ectasia and necrosis, extensive mucosal erosion to ulceration, and occasional complete loss and collapse of mucosal architecture (Fig. 2B) consistent with previous studies [42, 44, 47]. In contrast, colonic tissues from mice treated with either iMSC or adMSC exhibited an overall reduction in transmural inflammation, with significantly less infiltration of inflammatory cells in the lamina propria, diminished mucosal ulceration, and decreased mucosal collapse and granulation tissue formation. The overall histological
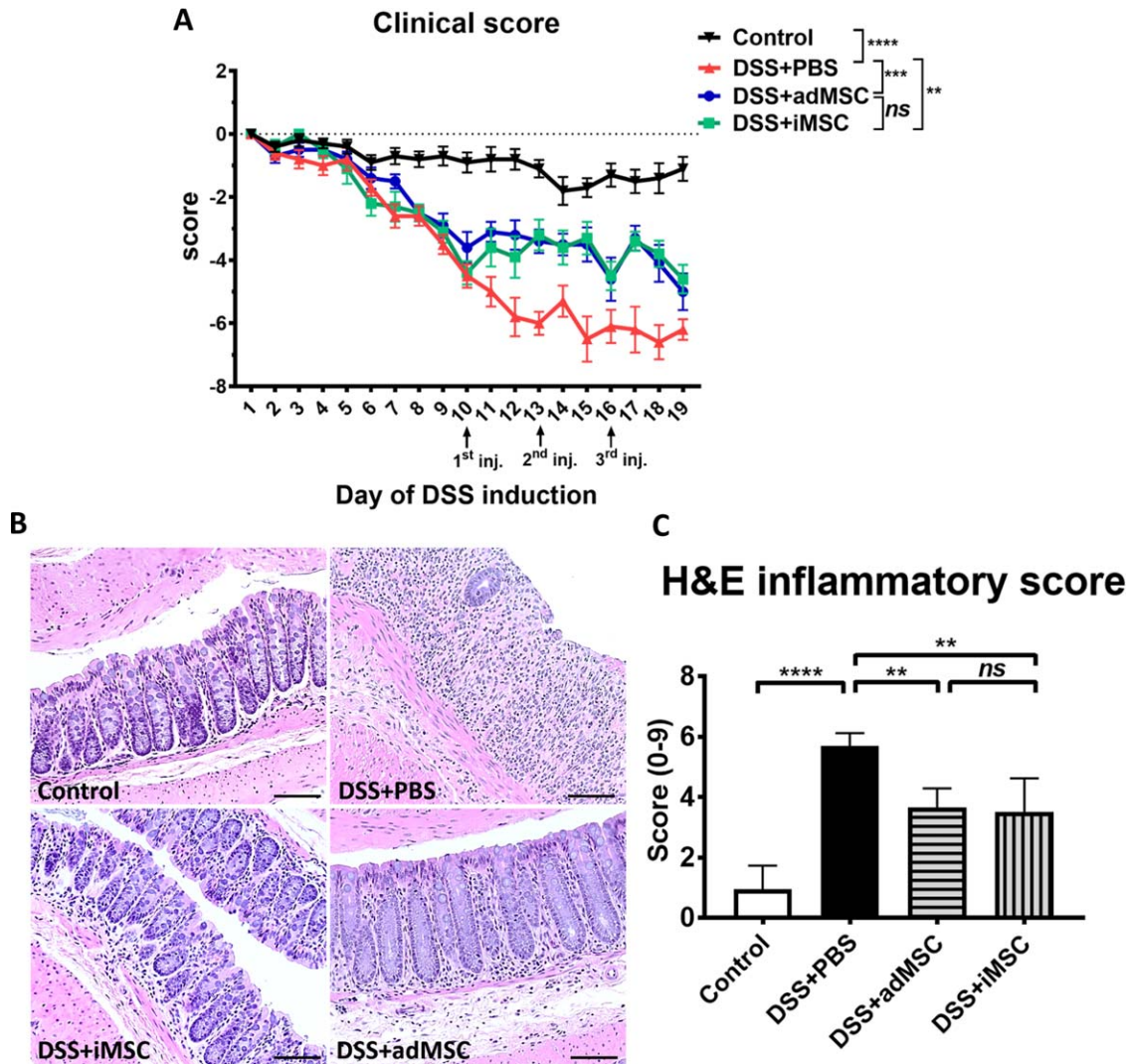
Figure 2. Effects of mesenchymal stem cells (MSC) administration on clinical scores and inflammatory score in DSS-induced colitis mice. Mice were monitored for percentage of weight loss, fecal occult blood, and fecal consistency every day during DSS treatment period (19 days) and a total clinical score was calculated. **(A):** Clinical score over time in 4 groups of mice ($n = 5$ per group): control, DSS treated + PBS; DSS + iMSC, and DSS + adMSC. MSC were administered by tail vein on days 10, 13, and 16. **(B):** Histology of colonic tissue sections from one mouse from each of 4 treatment groups, based on H&E stained sections. **(C):** Quantitative inflammatory scores assessed by H&E histopathology, as described in "Materials and Methods" section. Data was transformed to a normal distribution and the statistical differences were calculated using (A) repeated measures One-way ANOVA with Tukey's adjustment, (B) One-way ANOVA with Tukey's adjustment (*, $p \leq .05$; **, $p \leq .01$; ***, $p \leq .001$; ****, $p \leq .0001$). Scale bar indicated 50 μm. Abbreviations: adMSC, adipose-derived mesenchymal stem cell; DSS, dextran sodium sulfate; iMSC, iPSC-derived mesenchymal stem cells; inj, injection; ns, not significant; PBS, phosphate-buffered saline.

inflammatory scores were significantly improved in mice treated with either iMSC or adMSC, compared to the PBS-treated group (iMSC, $p = .002$; adMSC, $p = .003$) (Fig. 2C). These results indicated therefore that iMSC were equivalent to adMSC in their ability to ameliorate the signs of intestinal inflammation induced by DSS treatment in this model of IBD.

Trafficking of MSC to Intestinal and Extraintestinal Tissues

To investigate the distribution of MSCs to sites of colonic inflammation, MSC were labeled using DiR dye immediately prior to injection. Cell distribution was monitored using IVIS live animal imaging. These studies revealed that labeled MSCs were primarily distributed to lungs initially, and at later time points labeled MSC could also be localized in the liver and spleen (Fig. 3A). However,

labeled cells could not be detected by IVIS imaging in intestinal tissues.

To increase the sensitivity of cell detection, additional studies were done with mice injected with DiD-labeled MSC (Fig. 3B), followed by immunohistochemical examination of tissues from injected mice (Fig. 3C–3G). These studies revealed that labeled MSC could be detected only very rarely in the colonic mucosa and submucosa (Fig. 3D, 3E), in Peyer's patches (Fig. 3F, 3G) and mesenteric lymph nodes (Fig. 3C) of treated animals. In contrast, labeled MSC were much more numerous in the spleen (Fig. 3C) and lung tissues (data not shown). The relatively scarcity of MSC in colonic tissues following i.v. injection in DSS models is consistent with several previous studies [13, 22, 48, 49], but differs markedly from findings in other published studies in which high numbers of labeled MSC were found in intestinal tissues [23, 50,
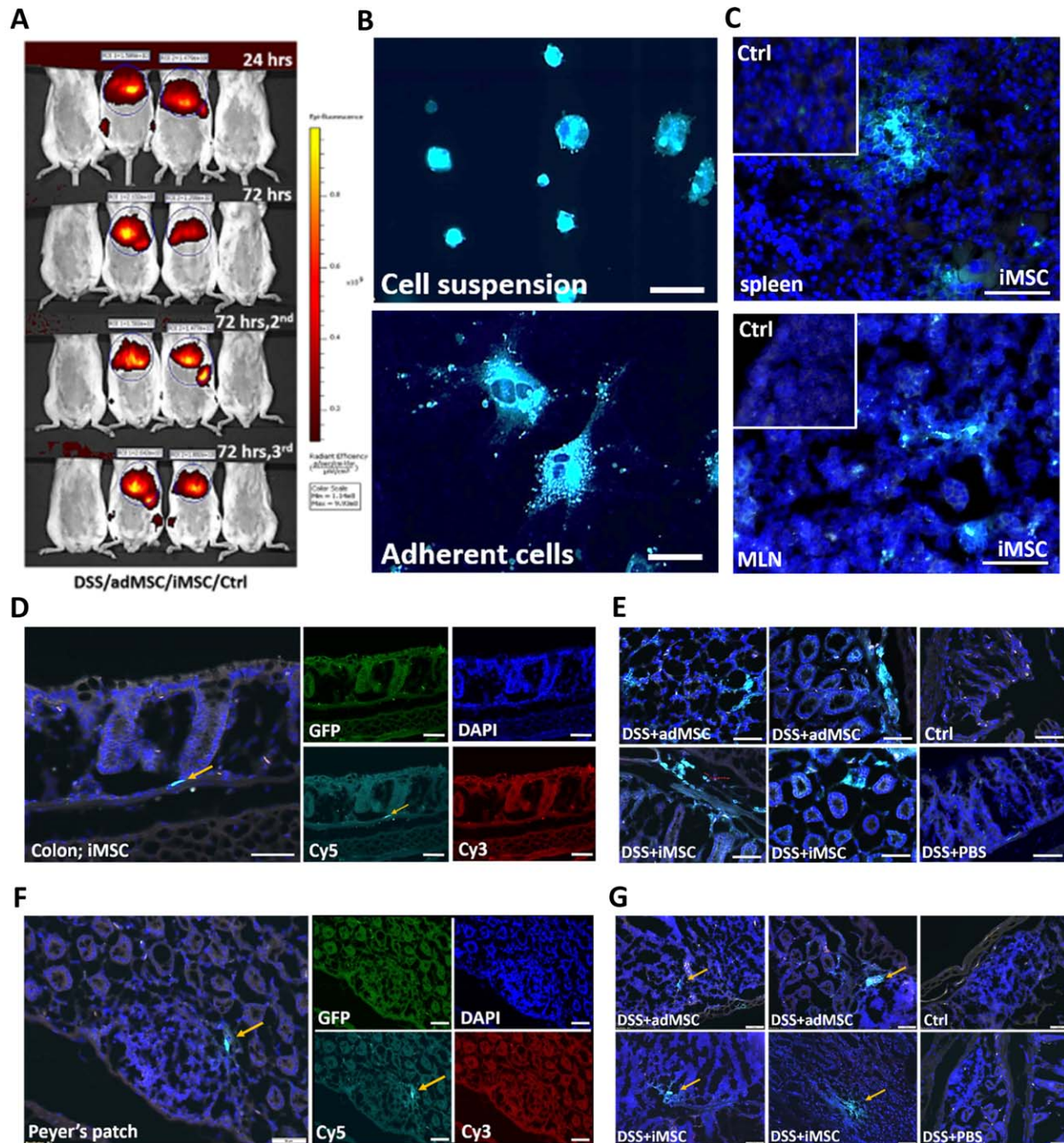
Figure 3. Localization of labeled mesenchymal stem cells (MSC) in live animals and tissue sections. **(A):** For in vivo localization, MSCs were labeled using DiR dye before injection and mice were monitored by IVIS in vivo fluorescent imaging at 24 hours after the first injection, 72 hours post-injections and on the day of euthanasia. High concentrations of MSC were found in lung and liver and spleen, but not in intestinal tissues. **(B):** In vitro labeled MSC using fluorescent labeled (DiD). Localization of labeled MSCs in colonic mucosa and regional lymphoid tissues, tissues were collected 10 days after MSC administration. **(C):** Presence of labeled MSCs in spleen and mesenteric lymph node tissues. **(D):** Labeled MSC in colonic mucosa (arrow) presented in corresponding channel. **(E):** High power views of labeled MSC in colonic mucosa and submucosa. **(F, G):** Labeled MSC in Peyer's patch of colon (arrow). Scale bar indicated 50 μm in all panels except panel (B) (indicated 25 μm). Abbreviations: adMSC, adipose-derived mesenchymal stem cell; Ctrl, control; DSS, dextran sodium sulfate; hrs, hours; iMSC, iPSC-derived mesenchymal stem cells; MLN, mesenteric lymph node; PBS, phosphate-buffered saline.

51]. Our findings, with very low numbers of MSC in colonic tissues, suggest that the therapeutic benefits of injected MSC were more likely to have been mediated by paracrine secreted factors than by direct cell-to-cell effects between MSC and colonic epithelial cells.

Effects of MSC Administration on Epithelial Regeneration

The histologic appearance of colonic tissue from mice treated with MSC demonstrated remarkable recovery of intestinal epithelial integrity (see Fig. 2B). These findings suggested therefore that
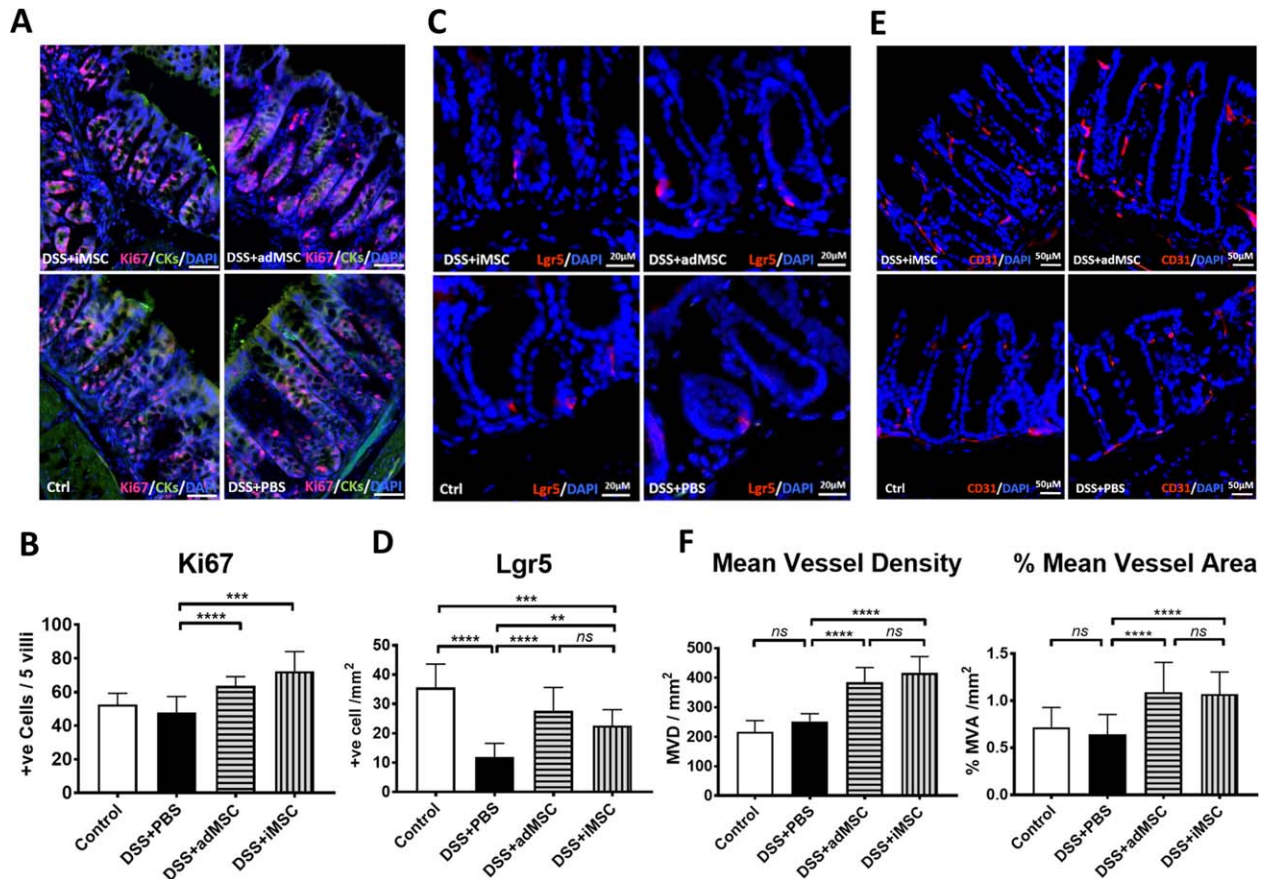
Figure 4. Effects of mesenchymal stem cells (MSC) administration on intestinal epithelial cell proliferation, stem cell recruitment, and angiogenesis. **(A):** Immunoflourescence detection of Ki-67+ (red) cytokeratin+ (green) intestinal epithelial cells in colonic tissues from mice with DSS-induced colitis, with or without MSC treatment. **(B):** Graphical representation of numbers of Ki-67+ epithelial cells/5 villi. **(C):** Immunofluorescence detection of Lgr5+ intestinal stem cells (red) at the base of colon crypts in colonic tissues from control and MSC-treated mice. **(D):** Graphical representation of numbers of Lgr5+ stem cells per mm^2 tissue. **(E):** Immunofluorescence detection of CD31+ neoangiogenic cells in colonic tissues of control and MSC treated mice. **(F):** Graphical representation of the mean vessel density and mean vessel area/mm^2 of mucosa, as determined as described in "Materials and Methods" section. The statistics reported as mean ± SD, statistical differences were calculated using One-way ANOVA with Tukey's adjustment (*, $p \leq .05$; **, $p \leq .01$; ***, $p \leq .001$; ****, $p \leq .0001$). Scale bar indicated 50 μm in all panels. Abbreviations: adMSC, adipose-derived mesenchymal stem cell; CKs, cytokeratin; DAPI, 4′,6-diamidino-2-phenylindole; DSS, dextran sodium sulfate; iMSC, iPSC-derived mesenchymal stem cells; Lgr5, leucine rich repeat containing G protein-coupled receptor 5; ns, not significant; PBS, phosphate-buffered saline.

MSC treatment may have affected directly the reconstitution of epithelial integrity in the colon. Stimulation of epithelial regeneration could be mediated by several factors, including enhanced neovascularization, increased intestinal stem cell regeneration, and greater crypt cell proliferation and differentiation [52, 53]. Therefore, immunohistochemistry was used to investigate these processes in colonic tissues of DSS-treated control mice and mice treated with iMSC and adMSC (Fig. 4).

First, we observed a significant increase in the numbers of Ki-67+ intestinal epithelial cells in the colon of mice treated with iMSC and with adMSC, compared to the numbers of Ki-67+ epithelial cells in DSS-only treated animals and in untreated control animals (Fig. 4A, 4B). In addition, we found that the numbers of Lgr5+ intestinal stem cells were significantly greater in the colonic mucosa of animals treated with MSC, compared to DSS-only treated or control animals (Fig. 4C, 4D). Finally, MSC-treated animals demonstrated increased angiogenesis as determined by significantly increased numbers of CD31+ endothelial cells, as well as increased mean vessel density and area compared to control animals, (Fig. 4E, 4F).

Taken together, these findings indicate that systemic administration of iMSC or adMSC exerted an important trophic effect on intestinal epithelial cells, by stimulating proliferation and recruitment of intestinal stem cells, and on the overall intestinal blood supply, by stimulating local angiogenesis. Thus, these findings suggest secretion of multiple trophic factors by i.v. delivered MSC. The stem cell tracking data, and the paucity of MSC detected in colonic tissues, strongly suggests that these trophic factors were likely to have been produced at sites distant from the GI tract.

Administration of MSC Reverses Microbiome Dysbiosis

Previous studies have found that DSS-induced colitis causes alterations in the gut microbiome [54]. In our studies, we used 16S sequencing to investigate the composition of the gut microbiome of DSS-treated animals, and we also found marked alterations in the populations of several important gut phyla (Fig. 5). For example, we observed a significant relative increase in *Proteobacteria* (Fig. 5A), along with increased *Bacteroides*, and decreased *Firmicutes* in mice treated with DSS, compared to untreated control animals (Fig. 5D). Overall, the DSS alone group had the least
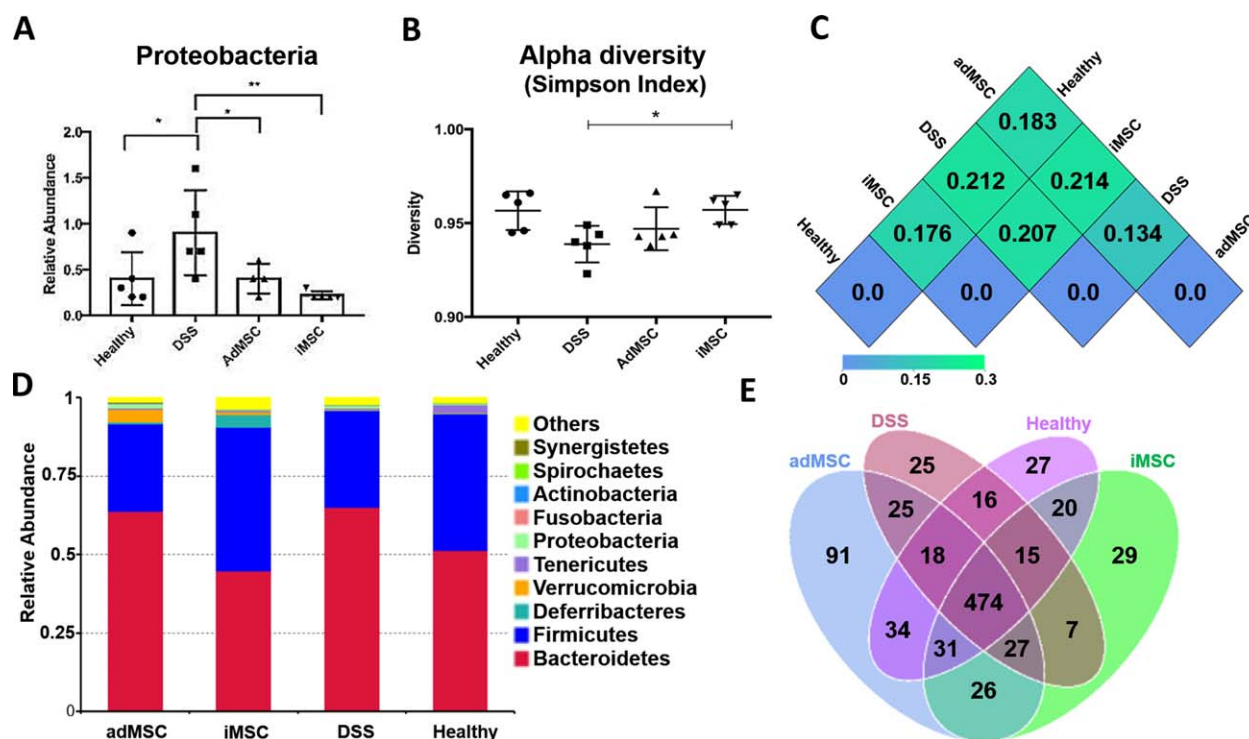
Figure 5. Effects of mesenchymal stem cells (MSC) administration on gut microbiome. Fecal pellets were collected at 2 days after the last MSC injection from control and MSC-treated animals ($n = 5$ per group) and analyzed by 16s rRNA sequencing as determined as described in "Materials and Methods" section. **(A):** Relative abundance of Proteobacteria presented in each treatment group. **(B):** Microbial diversity within treatment groups (Simpson alpha diversity index) calculated with QIIME (Version 1.7.0). **(C):** Comparative analysis of differences between treatment groups (beta diversity), heat map represents average differences, with 0 as no difference, 0.3 is maximum differences. Scale bar shown in bottom left. **(D):** Relative abundance of top 10 phyla presented in each treatment group. **(E):** Venn diagram generated according to the Operational Taxonomic Unit clustering of each treatment group, each number represents number of bacterial species, either shared or unique to treatment groups. The statistics reported as mean ± SD, statistical differences were calculated using One-way ANOVA with Tukey's adjustment (*, $p \leq .05$; **, $p \leq .01$; ***, $p \leq .001$; ****, $p \leq .0001$). Abbreviations: adMSC, adipose-derived mesenchymal stem cell; DSS, dextran sodium sulfate; iMSC, iPSC-derived mesenchymal stem cells.

microbial community diversity measured within a sample as showed in an alpha diversity graph (using Simpson index) (Fig. 5B). Also, as shown in the Venn diagram (Fig 5E); the iMSC and adMSC treated groups shared more OTUs (operational taxonomic units) with the healthy group compared to the DSS only group.

Notably, in mice treated with either iMSC or adMSC, after 10 days of stem cell treatment, and despite the continued administration of DSS, the composition of the microbiome in these animals had returned to a population that much more closely resembled that of the microbiome of healthy untreated mice (Fig. 5C). For example, the iMSC-treated group of animals had the most similar taxa distribution relative to heathy control animals, compared to DSS only animals or DSS animals treated with adMSC (Fig. 5D). These results suggest that treatment with MSC helped restore the normal colonic flora, although the exact mechanism of the effect remained undetermined.

Effects of MSC Administration on Intestinal Inflammation

The effects of MSC injection on inflammatory responses in the colon and regional lymphoid tissues were examined next. In colonic tissues of DSS-treated animals, increased infiltrates of F4/80+ and CD11b+ macrophages, CD3+, CD4+ T cells, and CD103+ inflammatory monocytes were observed, compared to colonic tissues of healthy untreated animals.

In animals treated with MSC, the numbers of macrophages and monocytes were significantly reduced compared to DSS only treated animals treated (Fig. 6A). FOXP3+ regulatory T cells were significantly more numerous in colonic tissues of mice treated with either iMSC or adMSC, compared to control animals or DSS-only animals (Fig. 6A). These results are consistent with the results of previous studies [13, 22] and suggest that MSC treatment ameliorated colonic inflammation, as reflected by increased numbers of regulatory T cells and reduced macrophage and neutrophil infiltration into colonic submucosa. However, MSC treatment in our model did not alter the numbers of infiltrating T cells in colonic tissues (Fig. 6A).

Notably, iMSC and adMSC were comparable in their effects on reducing the severity of colonic inflammation. However, there were no consistent changes in T cell or B cell or myeloid cell populations in the spleen or mesenteric lymph node tissues of animals treated with MSC, compared to animals with DSS-induced colitis (Fig. 6B). Thus, overall administration of MSC reduced local colonic inflammation, in addition to stimulating epithelial cell proliferation and angiogenesis, but had little effect on immune cell populations in extraintestinal tissues.

DISCUSSION

The use of MSCs to treat IBD has shown considerable promise in preclinical studies in rodent models, and in small clinical trials in
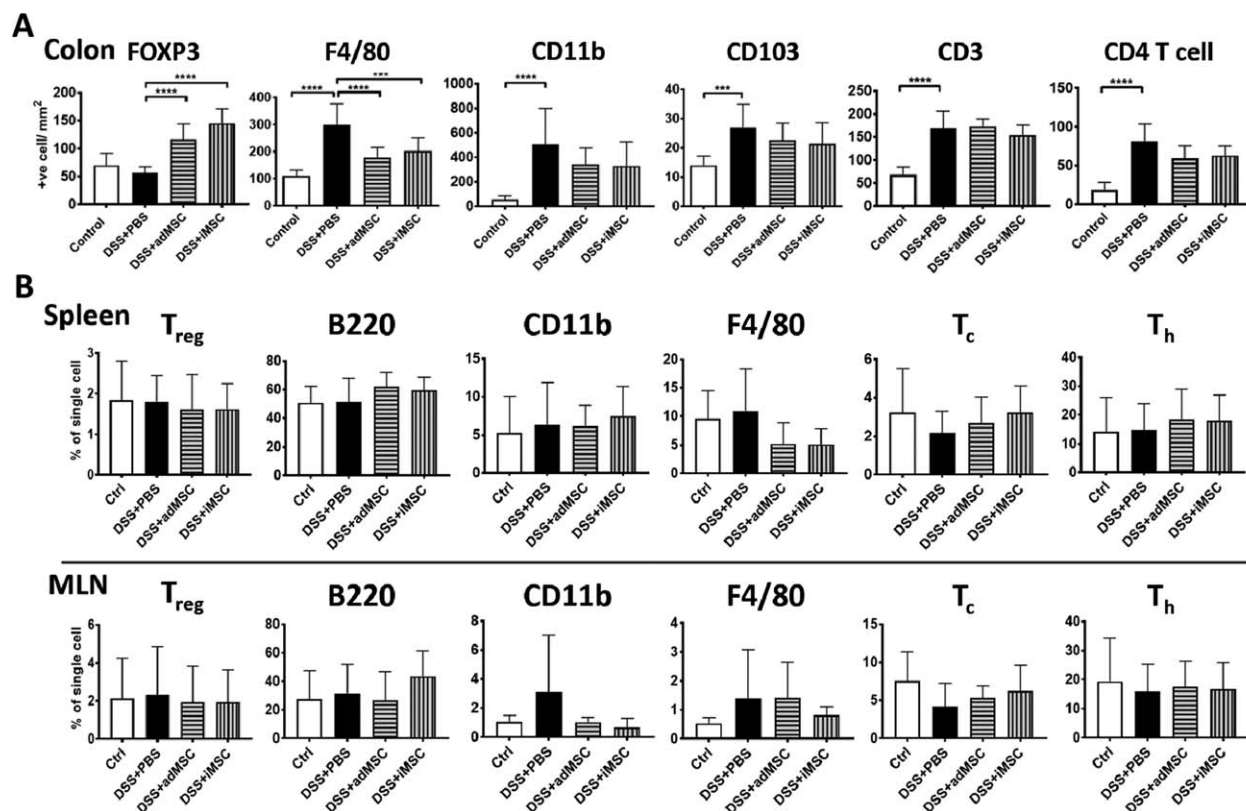
Figure 6. Effects of mesenchymal stem cells administration on colonic inflammation. Tissue sections were immunostained with the indicated antibodies, as noted in "Materials and Methods" section, and imaged using a confocal microscope. Quantitative image analysis was used to quantitate the density of inflammatory cells (see "Materials and Methods" section). **(A):** Distribution of FOXP3, F4/80, CD11b, CD3, CD4 T cell, and CD103+ cells in colonic tissues. **(B):** Leukocyte populations in spleen and mesenteric lymph node tissues as assessed by flow cytometry (see "Materials and Methods" section). Statistical differences were calculated using One-way ANOVA with Dunnett multiple comparison to DSS treated group (*, $p \leq .05$; **, $p \leq .01$; ***, $p \leq .001$; ****, $p \leq .0001$). Abbreviations: adMSC, adipose-derived mesenchymal stem cell; DAPI, 4′,6-diamidino-2-phenylindole; DSS, dextran sodium sulfate; FOXP3, Foxhead Box P3; iMSC, iPSC-derived mesenchymal stem cells; MLN, mesenteric lymph node; Tc, cytotoxic T cell; Th, T helper cell; Treg, regulatory T cell.

humans [13, 14, 17, 23, 32, 50, 55, 56]. However, the use of autologous or allogeneic bone marrow derived MSC or adMSC for larger scale clinical cellular therapy studies is subject to several important drawbacks, including the limited proliferative capacity of older MSC, donor-to-donor MSC variability, the costs associated with donor screening, and the time and expense associated with expanding MSC in primary culture [33, 36, 57]. Therefore, alternate cell sources for standardized and renewable, functional populations of MSC for cellular therapy are desirable. In the present study, we have investigated the potential for use of iMSC as an alternative source of cells for treatment of IBD. The potential advantages of iMSC for cellular therapy have been described previously [37, 38, 41, 58].

In our study, we found that iMSC were equivalent or in some cases superior to conventional adMSC for treatment of IBD, in terms of ameliorating clinical signs of colitis and stimulating intestinal healing. For example, the overall clinical score in DSS-treated mice was reduced by 26% at day 19 in mice treated with iMSC, compared to untreated mice (see Fig. 2A), while the reduction in clinical score was 19% in mice treated with adMSC. In addition, intestinal inflammation was reduced equivalently in mice treated with iMSC versus mice treated with adMSC (see Fig. 2C). Also, iMSC administration elicited significant stimulation of intestinal epithelial cell proliferation, increased in the numbers of Lgr5+ intestinal stem cells, and increased in intestinal angiogenic

responses (see Fig. 4). Notably, in our study the long-term therapeutic effect was maintained by repeated MSC injections, suggesting a relatively short duration of action following a single MSC administration [59, 60].

The anti-inflammatory properties of MSC have been described previously, and these effects certainly may account for a portion of the overall beneficial effect of MSC on colitis. For example, studies have shown that MSC suppresses Th17 responses, increase the Treg: Th17 ratio, and lead to loss of effector T cells [61–64]. In addition, our study suggests alternative mechanisms by which MSC may also exert an important effect on resolution of lesions in the gut associated with IBD. For example, stimulation of epithelial regeneration may be as important to healing as suppression of inflammation. The significant increase in the number of Lgr5+ intestinal stem cells observed in the epithelium of mice treated with iMSC or adMSC, compared to control DSS mice (see Fig. 4C, 4D), is indicative of stimulation of local stem cell proliferation and/or recruitment. Our results are in agreement with previous studies of radiation-induced GI injury which suggest that MSC may secrete molecules leading to activation of the Wnt/β-catenin signaling pathway required for Lgr5+ cell proliferation [27]. Also reduced inflammatory cytokines may improve self-renewal or return normal differentiation or apoptotic rate of Lgr5+ cells [65, 66]. Therefore, suppression of inflammation and stimulation of local stem cell proliferation by MSC may work together

synergistically to stimulate intestinal healing. Furthermore, we observed significantly greater proliferation of mature epithelial cells in the colonic mucosa, consistent with a stimulatory effect of MSC secreted factors. Given the rather sparse distribution of MSC found in the colonic mucosa or submucosa (see Fig. 3D, 3E), this MSC effect is most likely mediated by trophic factors secreted by MSC residing in extraintestinal tissues, including the lung and spleen. Finally, we also observed that angiogenic responses were significantly enhanced locally in colonic tissues in animals treated with MSC, consistent with the release of proangiogenic cytokines such as VEGF, as has been reported previously [67].

A second potential mechanism of intestinal healing by MCS involves microbiome alterations. The gut microbiome is known to exert an important stimulatory effect on intestinal integrity and local immune responses [68]. For example, intestinal healing has been shown to be significantly impaired in mice in which the microbiome has been disrupted, and in mice unable to sense intestinal bacteria due to disrupted TLR signaling [69, 70]. In the present study, we observed that the microbiome alterations induced by DSS injury were to a large degree reversed by the administration of MSC, including administration of either iMSC or adMSC (see Fig. 5). For example, the diversity of the gut microbiome phyla was significantly increased in MSC-treated animals, compared to DSS only treated animals (Fig. 5B). These findings suggest therefore that by generating a more diverse microbiome more closely resembling that of healthy control animals, MSC administration improved overall intestinal health and healing.

However, it should also be acknowledged that is not clear whether the microbiome changes were a consequence of improved intestinal healing, or whether intestinal healing resulted from the improved microbiome. More likely, both mechanisms were likely to have been operative, with MSC-induced changes in the colonic epithelium altering the microbiome, and the microbiome changes further stimulating intestinal epithelial regeneration and angiogenesis.

In summary, our studies reveal that iMSC are equally effective as adMSC when administered systemically for resolving IBD in a rodent model, without inducing detectable adverse effects, even after repeated i.v. administration. Moreover, the effects of MSC on IBD appear to be multifactorial, involving both improved intestinal epithelial regeneration, beneficial microbiome alterations, and suppression of intestinal inflammation. To evaluate the safety and efficacy of iMSC for treatment of IBD in a more translationally relevant setting, we have initiated studies of iMSC treatment in a spontaneous IBD model in pet dogs, based on early evidence of efficacy of MSC efficacy in a similar model [16]. Moreover, we have recently conducted safety studies for systemically administered canine iMSC in dogs and found no evidence of teratoma or tumor formation (L. Chow et al., manuscript submitted for publication). Thus, the use of systemically administered iMSC as a new cellular therapy is an option for management of refractory IBD, provided regulatory and potential safety issues can be adequately addressed.

CONCLUSION

These studies are the first to demonstrate the equivalence of iMSC and adMSC for treatment of IBD, in a widely used rodent DSS colitis model. In all aspects evaluated, iMSC were equally potent in terms of suppressing intestinal inflammation and stimulating intestinal healing. These studies also revealed a significant stimulatory effect of iMSC cellular therapy on epithelial proliferation and angiogenesis, and restoration of normal microbiome populations.

ACKNOWLEDGMENTS

AUTHOR CONTRIBUTIONS

S.S., L.C., and S.D.: conception and design, provision of study material, collection and assembly of data, data analysis and interpretation, manuscript writing, final approval of manuscript; V.J., J.C., W.W., and D.R.: collection and assembly of data; S.D.: conception and design, financial support, manuscript writing, final approval of manuscript.

DISCLOSURE OF POTENTIAL CONFLICTS OF INTEREST

The authors indicated no potential conflicts of interest.

REFERENCES

1 Xavier RJ, Podolsky DK. Unravelling the pathogenesis of inflammatory bowel disease. Nature 2007;448:427–434.

2 Torres J, Mehandru S, Colombel J-F et al. Crohn's disease. Lancet 2017;389:1741–1755.

3 Ungaro R, Mehandru S, Allen PB et al. Ulcerative colitis. Lancet 2017;389:1756–1770.

4 Hendrickson BA, Gokhale R, Cho JH. Clinical aspects and pathophysiology of inflammatory bowel disease. Clin Microbiol Rev 2002; 15:79–94.

5 Magro F, Langner C, Driessen A et al. European consensus on the histopathology of inflammatory bowel disease. J Crohns Colitis 2013;7:827–851.

6 Chow L, Johnson V, Coy J et al. Mechanisms of immune suppression utilized by canine adipose and bone marrow-derived mesenchymal stem cells. Stem Cells Dev 2017; 26:374–389.

7 Wheat WH, Chow L, Kurihara JN et al. Suppression of canine dendritic cell activation/maturation and inflammatory cytokine release by mesenchymal stem cells occurs through multiple distinct biochemical pathways. Stem Cells Dev 2017;26:249–262.

8 Gao F, Chiu SM, Motan DAL et al. Mesenchymal stem cells and immunomodulation: Current status and future prospects. Cell Death Dis 2016;7:e2062.

9 Bouffi C, Bony C, Courties G et al. IL-6-dependent PGE2 secretion by mesenchymal stem cells inhibits local inflammation in experimental arthritis. PLoS One 2010;5:e14247.

10 Chiossone L, Conte R, Spaggiari GM et al. Mesenchymal stromal cells induce peculiar alternatively activated macrophages capable of dampening both innate and adaptive immune responses. STEM CELLS 2016;34:1909–1921.

11 Anderson P, Souza-Moreira L, Morell M et al. Adipose-derived mesenchymal stromal cells induce immunomodulatory macrophages which protect from experimental colitis and sepsis. Gut 2013;62:1131–1141.

12 Liang L, Dong C, Chen X et al. Human umbilical cord mesenchymal stem cells ameliorate mice trinitrobenzene sulfonic acid (TNBS)-induced colitis. Cell Transplant 2011;20:1395–1408.

13 Park JS, Yi TG, Park JM et al. Therapeutic effects of mouse bone marrow-derived clonal mesenchymal stem cells in a mouse model of inflammatory bowel disease. J Clin Biochem Nutr 2015;57:192–203.

14 Lee HJ, Oh S-H, Jang HW et al. Long-term effects of bone marrow-derived mesenchymal

stem cells in dextran sulfate sodium-induced murine chronic colitis. Gut Liver 2016;10:412–419.

15 Hoffman AM, Dow SW. Concise review: Stem cell trials using companion animal disease models. Stem Cells 2016;34:1709–1729.

16 Pérez-Merino EM, Usón-Casaús JM, Zaragoza-Bayle C et al. Safety and efficacy of allogeneic adipose tissue-derived mesenchymal stem cells for treatment of dogs with inflammatory bowel disease: Clinical and laboratory outcomes. Vet J 2015;206:385–390.

17 Duijvestein M, Vos AC, Roelofs H et al. Autologous bone marrow-derived mesenchymal stromal cell treatment for refractory luminal Crohn's disease: Results of a phase I study. Gut 2010;59:1662–1669.

18 Mannon PJ. Remestemcel-L: Human mesenchymal stem cells as an emerging therapy for Crohn's disease. Expert Opin Biol Ther 2011;11:1249–1256.

19 Hospital to Academy of Military Medical Sciences. Human Umbilical Cord Derived Mesenchymal Stem Cell Therapy in Active Ulcerative Colitis. Available at https://ClinicalTrials.gov/show/NCT02442037. Accessed May 6, 2015.

20 Forbes GM, Sturm MJ, Leong RW et al. A phase 2 study of allogeneic mesenchymal stromal cells for luminal Crohn's disease refractory to biologic therapy. Clin Gastroenterol Hepatol 2014;12:64–71.

21 Hu J, Zhao G, Zhang L et al. Safety and therapeutic effect of mesenchymal stem cell infusion on moderate to severe ulcerative colitis. Exp Ther Med 2016;12:2983–2989.

22 Sala E, Genua M, Petti L et al. Mesenchymal stem cells reduce colitis in mice via release of TSG6, independently of their localization to the intestine. Gastroenterology 2015;149:163–176.e120.

23 Gonzalez-Rey E, Andreson P, Gonzalez MA et al. Human adult stem cells derived from adipose tissue protect against experimental colitis and sepsis. Gut 2009;58:929–939.

24 Takeyama H, Mizushima T, Uemura M et al. Adipose-derived stem cells ameliorate experimental murine colitis via TSP-1-dependent activation of latent TGF-β. Dig Dis Sci 2017;62:1963–1974.

25 Semont A, Mouiseddine M, Francois A et al. Mesenchymal stem cells improve small intestinal integrity through regulation of endogenous epithelial cell homeostasis. Cell Death Differ 2010;17:952–961.

26 Tanaka H, Arimura Y, Yabana T et al. Myogenic lineage differentiated mesenchymal stem cells enhance recovery from dextran sulfate sodium-induced colitis in the rat. J Gastroenterol 2011;46:143–152.

27 Gong W, Guo M, Han Z et al. Mesenchymal stem cells stimulate intestinal stem cells to repair radiation-induced intestinal injury. Cell Death Dis 2016;7:e2387.

28 Linard C, Busson E, Holler V et al. Repeated autologous bone marrow-derived mesenchymal stem cell injections improve radiation-induced proctitis in pigs. Stem Cells Translational Medicine 2013;2:916–927.

29 Sémont A, Demarquay C, Bessout R et al. Mesenchymal stem cell therapy stimulates endogenous host progenitor cells to improve colonic epithelial regeneration. PLoS One 2013;8:e70170.

30 Swenson ES, Theise ND. Stem cell therapeutics: Potential in the treatment of inflammatory bowel disease. Clin Exp Gastroenterol 2010;3:1–10.

31 Ren G, Chen X, Dong F et al. Concise review: Mesenchymal stem cells and translational medicine: Emerging issues. Stem Cells Translational Medicine 2012;1:51–58.

32 Molendijk I, Bonsing BA, Roelofs H et al. Allogeneic bone marrow-derived mesenchymal stromal cells promote healing of refractory perianal fistulas in patients with Crohn's disease. Gastroenterology 2015;149:918–927.e916.

33 Stolzing A, Jones E, McGonagle D et al. Age-related changes in human bone marrow-derived mesenchymal stem cells: Consequences for cell therapies. Mech Ageing Dev 2008;129:163–173.

34 Duscher D, Rennert RC, Januszyk M et al. Aging disrupts cell subpopulation dynamics and diminishes the function of mesenchymal stem cells. Sci Rep 2014;4:7144.

35 Griffin MD, Ritter T, Mahon BP. Immunological aspects of allogeneic mesenchymal stem cell therapies. Hum Gene Ther 2010;21:1641–1655.

36 Nitkin CR, Bonfield TL. Concise review: Mesenchymal stem cell therapy for pediatric disease: Perspectives on success and potential improvements. Stem Cells Translational Medicine 2017;6:539–565.

37 Jung Y, Bauer G, Nolta JA. Concise review: Induced pluripotent stem cell-derived mesenchymal stem cells: Progress toward safe clinical products. Stem Cells 2012;30:42–47.

38 Lian Q, Zhang Y, Zhang J et al. Functional mesenchymal stem cells derived from human induced pluripotent stem cells attenuate limb ischemia in mice. Circulation 2010;121:1113–1123.

39 Wei H, Tan G, Manasi et al. One-step derivation of cardiomyocytes and mesenchymal stem cells from human pluripotent stem cells. Stem Cell Res 2012;9:87–100.

40 Lai P-L, Lin H, Chen S-F et al. Efficient generation of chemically induced mesenchymal stem cells from human dermal fibroblasts. Sci Rep 2017;7:44534.

41 Sun YQ, Deng MX, He J et al. Human pluripotent stem cell-derived mesenchymal stem cells prevent allergic airway inflammation in mice. Stem Cells 2012;30:2692–2699.

42 Chassaing B, Aitken JD, Malleshappa M et al. Dextran sulfate sodium (DSS)-induced colitis in mice. Curr Protoc Immunol 2014;104:Unit-15.25.

43 Wirtz S, Neufert C, Weigmann B et al. Chemically induced mouse models of intestinal inflammation. Nat Protoc 2007;2:541–546.

44 Erben U, Loddenkemper C, Doerfel K et al. A guide to histomorphological evaluation of intestinal inflammation in mouse models. Int J Clin Exp Pathol 2014;7:4557–4576.

45 Schneider CA, Rasband WS, Eliceiri KW. NIH image to ImageJ: 25 years of image analysis. Nat Methods 2012;9:671–675.

46 Dominici M, Le Blanc K, Mueller I et al. Minimal criteria for defining multipotent mesenchymal stromal cells. The International Society for Cellular Therapy position statement. Cytotherapy 2006;8:315–317.

47 Banerjee A, Bizzaro D, Burra P et al. Umbilical cord mesenchymal stem cells modulate dextran sulfate sodium induced acute colitis in immunodeficient mice. Stem Cell Res Ther 2015;6:79.

48 Duijvestein M, Wildenberg ME, Welling MM et al. Pretreatment with interferon-γ enhances the therapeutic activity of mesenchymal stromal cells in animal models of colitis. Stem Cells 2011;29:1549–1558.

49 Parekkadan B, Tilles AW, Yarmush ML. Bone marrow-derived mesenchymal stem cells ameliorate autoimmune enteropathy independently of regulatory t cells. Stem Cells 2008;26:1913–1919.

50 Tanaka F, Tominaga K, Ochi M et al. Exogenous administration of mesenchymal stem cells ameliorates dextran sulfate sodium-induced colitis via anti-inflammatory action in damaged tissue in rats. Life Sci 2008;83:771.

51 Hayashi Y, Tsuji S, Tsujii M et al. The transdifferentiation of bone-marrow-derived cells in colonic mucosal regeneration after dextran-sulfate-sodium-induced colitis in mice. Pharmacology 2007;80:193–199.

52 Ando Y, Inaba M, Sakaguchi Y et al. Subcutaneous adipose tissue-derived stem cells facilitate colonic mucosal recovery from 2,4,6-trinitrobenzene sulfonic acid (TNBS)-induced colitis in rats. Inflamm Bowel Dis 2008;14:826–838.

53 Stappenbeck TS, Miyoshi H. The role of stromal stem cells in tissue regeneration and wound repair. Science 2009;324:1666–1669.

54 Mar JS, Nagalingam NA, Song Y et al. Amelioration of DSS-induced murine colitis by VSL#3 supplementation is primarily associated with changes in ileal microbiota composition. Gut Microbes 2014;5:494–503.

55 Garcia-Olmo D, Herreros D, Pascual I et al. Expanded adipose-derived stem cells for the treatment of complex perianal fistula: A phase II clinical trial. Dis Colon Rectum 2009;52:79–86.

56 de la Portilla F, Alba F, García-Olmo D et al. Expanded allogeneic adipose-derived stem cells (eASCs) for the treatment of complex perianal fistula in Crohn's disease: results from a multicenter phase I/IIa clinical trial. Int J Colorectal Dis 2013;28:313–323.

57 Zhang J, Huang X, Wang H et al. The challenges and promises of allogeneic mesenchymal stem cells for use as a cell-based therapy. Stem Cell Res Ther 2015;6:234.

58 Hynes K, Menicanin D, Mrozik K et al. Generation of functional mesenchymal stem cells from different induced pluripotent stem cell lines. Stem Cells Dev 2014;23:1084–1096.

59 Nemeth K, Leelahavanichkul A, Yuen PS et al. Bone marrow stromal cells attenuate sepsis via prostaglandin E(2)-dependent reprogramming of host macrophages to increase their interleukin-10 production. Nat Med 2009;15:42–49.

60 Parekkadan B, Milwid JM. Mesenchymal stem cells as therapeutics. Annu Rev Biomed Eng 2010;12:87–117.

61 Ghannam S, Pène J, Torcy-Moquet G et al. Mesenchymal stem cells inhibit human Th17 cell differentiation and function and induce a T regulatory cell phenotype. J Immunol 2010;185:302–312.

62 Luz-Crawford P, Kurte M, Bravo-Alegría J et al. Mesenchymal stem cells generate a

CD4(+)CD25(+)Foxp3(+) regulatory T cell population during the differentiation process of Th1 and Th17 cells. Stem Cell Res Ther 2013;4:65.

63 Duffy MM, Ritter T, Ceredig R et al. Mesenchymal stem cell effects on T-cell effector pathways. Stem Cell Res Ther 2011;2:34.

64 Plumas J, Chaperot L, Richard MJ et al. Mesenchymal stem cells induce apoptosis of activated T cells. Leukemia 2005;19:1597–1604.

65 Delgado ME, Grabinger T, Brunner T. Cell death at the intestinal epithelial front line. FEBS J 2016;283:2701–2719.

66 Neal MD, Richardson WM, Sodhi CP et al. Intestinal stem cells and their roles during mucosal injury and repair. J Surg Res 2011; 167:1–8.

67 Song S-Y, Chung H-M, Sung J-H. The pivotal role of VEGF in adipose-derived-stem-cell-mediated regeneration. Expert Opin Biol Ther 2010;10:1529–1537.

68 Sommer F, Bäckhed F. The gut microbiota–masters of host development and physiology. Nat Rev Microbiol 2013;11:227.

69 Abreu MT. Toll-like receptor signalling in the intestinal epithelium: How bacterial recognition shapes intestinal function. Nat Rev Immunol 2010;10:131–144.

70 Brown SL, Riehl TE, Walker MR et al. Myd88-dependent positioning of Ptgs2-expressing stromal cells maintains colonic epithelial proliferation during injury. J Clin Invest 2007;117:258–269.

See www.StemCellsTM.com for supporting information available online.